

Shaken *and* stirred: Random organization reduces viscosity and dissipation in granular suspensions

SUPPLEMENTARY INFORMATION

Christopher Ness,¹ Romain Mari,^{2,3} and Michael E. Cates²

¹*Department of Chemical Engineering and Biotechnology,
University of Cambridge, Cambridge CB3 0AS, United Kingdom*

²*DAMTP, Centre for Mathematical Sciences, University of Cambridge, Cambridge CB3 0WA, United Kingdom*

³*Université Grenoble Alpes, CNRS, LIPhy, 38000 Grenoble, France*

(Dated: May 9, 2022)

I. DEMONSTRATION THAT OUR NUMERICAL MODEL PREDICTS $\mu(J)$ RHEOLOGY

We demonstrate in Figure S1 that our numerical model generates results that are qualitatively consistent with viscous number “ $\mu(J)$ ” rheology as motivated by the experimental work of Boyer *et al.* [F. Boyer, É. Guazzelli, and O. Pouliquen, “Unifying suspension and granular rheology”, *Physical Review Letters* 107, 188301 (2011)]. The ratio between the shear stress and the pressure ($\mu = \tau/P$), and the volume fraction ϕ , are shown therein to be describable simply as functions of the viscous number, which is defined as $J = \eta\dot{\gamma}/P$ for suspending fluid viscosity η and shear rate $\dot{\gamma}$. Some sources of quantitative discrepancy between our numerical result and the empirical model based on Boyer’s experiment are variations in polydispersity and in the particle-particle friction coefficient. These quantities influence the numerical values of both the critical volume fraction and the limiting stress ratio measured when $J \rightarrow 0$. Moreover, the finite particle hardness used in this work allows the critical volume fraction to be exceeded when P becomes large. In our model, we have chosen to simulate a binary mixture of particles with diameter ratio 1:1.4, principally to avoid crystallisation. We used a particle-particle static friction coefficient of 1.

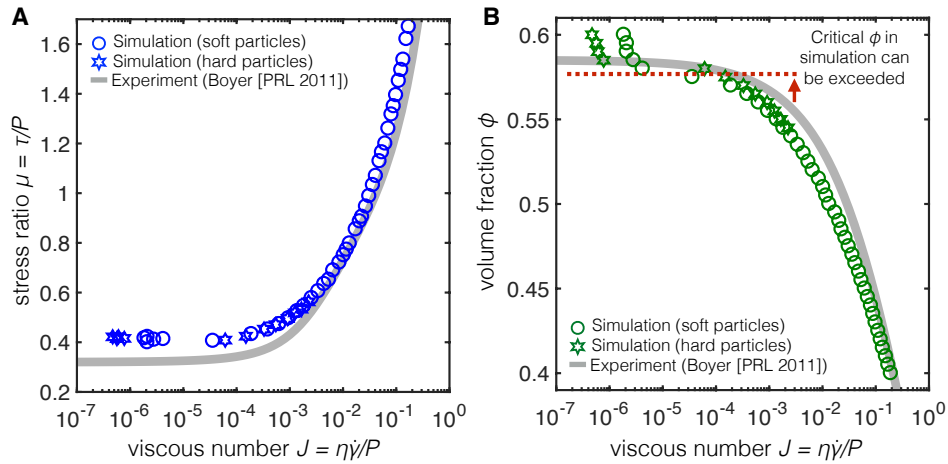


FIG. S1. Comparison of the results from the present model to viscous number rheology. We compare our numerical results obtained while operating under simple shear without oscillations (using direct force calculation) with fits to the empirical model proposed by Boyer *et al.*, using their parameters. Shown as functions of the viscous number $J = \eta\dot{\gamma}/P$ are the stress ratio $\mu = \tau/P$ (A) and the volume fraction ϕ (B) for two values of the particle hardness.

II. INFLUENCE OF PRIMARY-CROSS SHEAR OCS PHASE DIFFERENCE

The superimposed oscillations in the primary and cross-shear directions are given respectively by $\gamma^{\text{pri}}(t) = \gamma \sin(\omega^{\text{pri}}t + \delta) + \dot{\gamma}t$ and $\gamma^{\text{OCS}}(t) = \gamma \sin(\omega t)$, leading to the control parameters $\omega^{\text{pri}}\gamma/\dot{\gamma}$, $\omega\gamma/\dot{\gamma}$ and the phase shift δ . In Figure 1B of the main article we presented data showing the variation of the relative viscosity η_r with $\omega^{\text{pri}}\gamma/\dot{\gamma}$ and $\omega\gamma/\dot{\gamma}$. In Figure S2 we demonstrate that this result is insensitive to the phase angle δ .

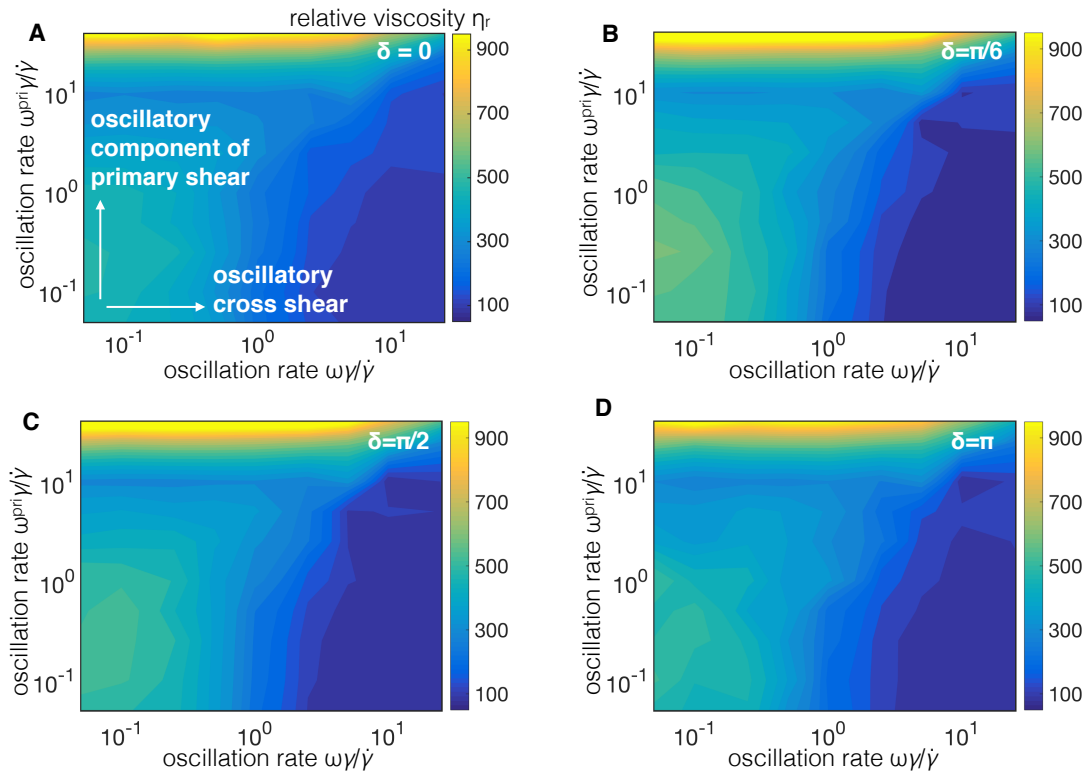


FIG. S2. Viscosity maps analogous to Figure 1B of the main article but with varying phase shift δ . Shown are phase shifts $\delta = 0$ (A), $\pi/6$ (B), $\pi/2$ (C) and π (D). The viscosity in the primary shear direction is highly sensitive to the oscillatory frequencies in primary and OCS, but rather insensitive to the phase angle δ .

III. TIME EVOLUTION OF THE RELATIVE VISCOSITY FOR THE SO AND AO PROTOCOLS

Shown in Figure S3 are the time evolutions of the relative primary viscosity η_r and particle-particle contact number while switching off the Simple OCS (SO) protocol and the relative primary viscosity for switching on-and-off the Alternating OCS (AO) protocol. For the SO protocol, a finite strain is required to reconstruct the contact network (and hence the contact stress) if we suddenly switch off the oscillations during a well-developed SO flow, illustrated in Figure S3 A, B. The necessary strain increases with the rate $\omega\gamma/\dot{\gamma}$ at which we were oscillating the material previously. In particular, when we ‘make more room’ using faster oscillations we have to strain further to bring particles back together after switching off the oscillations. In Figure S3 C we present the time evolution of the relative viscosity while switching the AO protocol on-and-off. Switching AO on leads quickly to a drop in the relative viscosity. Within

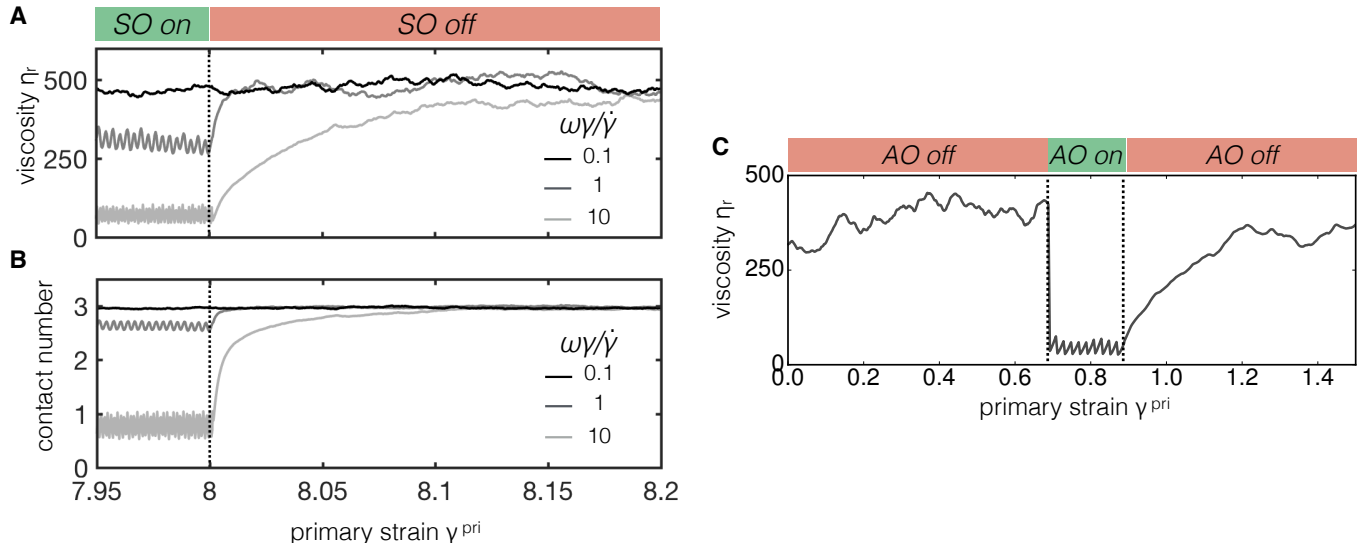


FIG. S3. Time evolution of the viscosity for the SO and AO protocols. Shown are the time evolution of the relative viscosity (A) and particle-particle contact number (B) after switching off oscillating flow in the simple OCS (SO) protocol. Also shown is the time evolution of the relative viscosity when switching on-and-off the oscillating flow in the Alternating OCS (AO) protocol (C).

the “AO on” phase, we see sawtooth-like evolution of the viscosity with the abrupt rises in viscosity quickly being truncated by the regular alternating periods of transverse flow (we used $n = 1$ period of oscillation per AO cycle, and $\gamma = \Gamma = 1$), keeping the time-averaged viscosity low. After switching off AO, the relative viscosity returns to its steady shear value over a primary strain of $\gamma^{\text{pri}} \approx 0.2$, comparable to that observed when switching off SO (Figure S3 A).

IV. SETTING THE VISCOSITY USING A PROPORTIONAL FLOW CONTROLLER

It is found that the transient response of the viscosity to switching on SO flow occurs over $\mathcal{O}(10)$ oscillations, while the response to switching off SO occurs for primary strains $\gamma_{xy} = \mathcal{O}(0.01) - \mathcal{O}(0.1)$, depending on the extent of room-making that was achieved under the preceding value of $\omega\gamma/\dot{\gamma}$. This suggests that we might implement a feedback loop that actively adjusts ω as a function of time in order to achieve a target viscosity. Such a procedure might be useful, for example, in extrusion processes to maintain steady flow or to allow pumps to operate within narrow bounds. We numerically implement a simplistic proportional controller and find that it can achieve target viscosities within strains of order 1. The current relative viscosity of the material $\eta_r(t)$ is measured at intervals within the response time mentioned above. In this case we chose to measure the viscosity at intervals of $0.01\dot{\gamma}t$. A target viscosity is defined as η^\dagger . The material is sheared in the primary direction at rate $\dot{\gamma}$ and we set an initial SO period of P_0 . The period is then updated at the aforementioned time intervals according to $P_{t+1} = P_t + K_p(\eta^\dagger - \eta_r(t))$. The results of such a control system are illustrated in Figure S4 for two different target viscosities, showing that target viscosities can be achieved within overall primary strains of $\mathcal{O}(1)$. The minimum and maximum viscosities that can be achieved by this protocol are set according to Figure 1 of the main text.

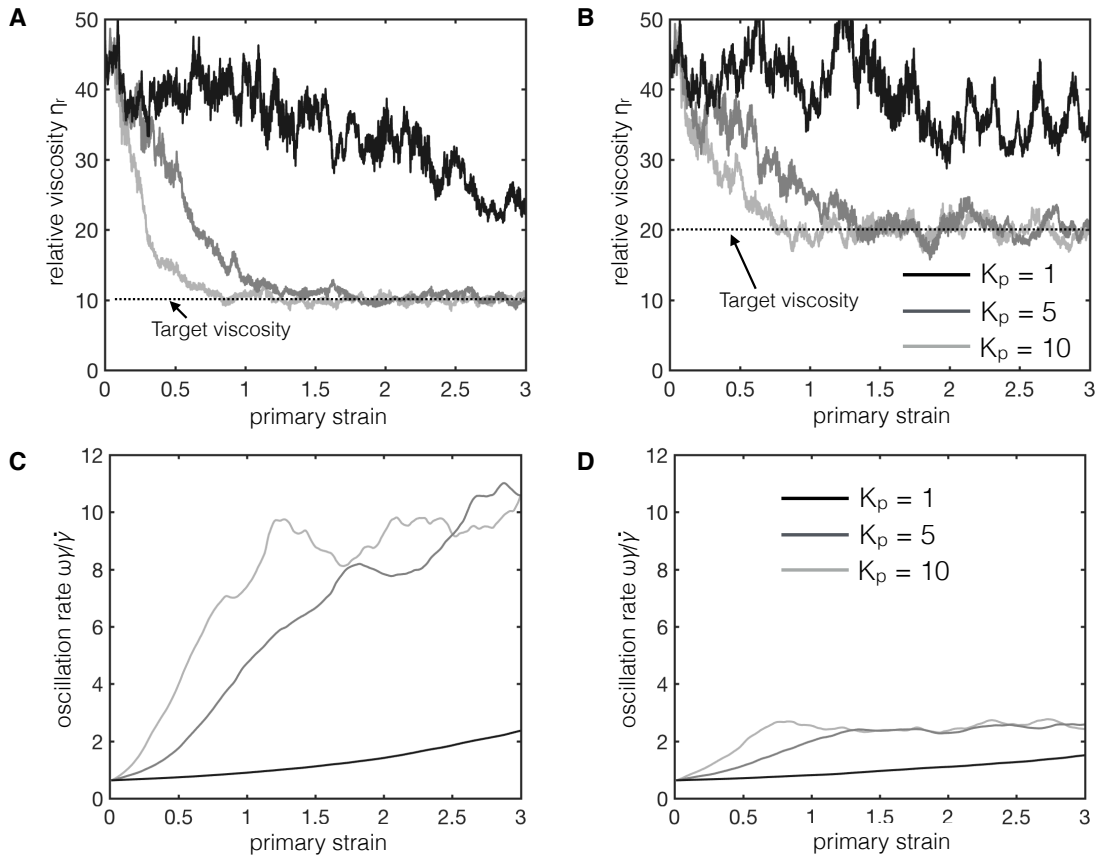


FIG. S4. Time evolution of the relative viscosity under proportional control in the SO protocol. Shown are data for set point relative viscosities $\eta^\dagger = 10$ (**A**) and $\eta^\dagger = 20$ (**B**) as well as the time evolution of the control variable $\omega\gamma/\gamma$ for $\eta^\dagger = 10$ (**C**) and $\eta^\dagger = 20$ (**D**). We used three different values of the proportional term K_p .